SUPPLEMENTARY FIGURES

Delmas *et al*

““WIF1 is a Frequent Target for Epigenetic Silencing in Squamous Cell Carcinoma of the Cervix”

(*CARCIN-2011-00210*).

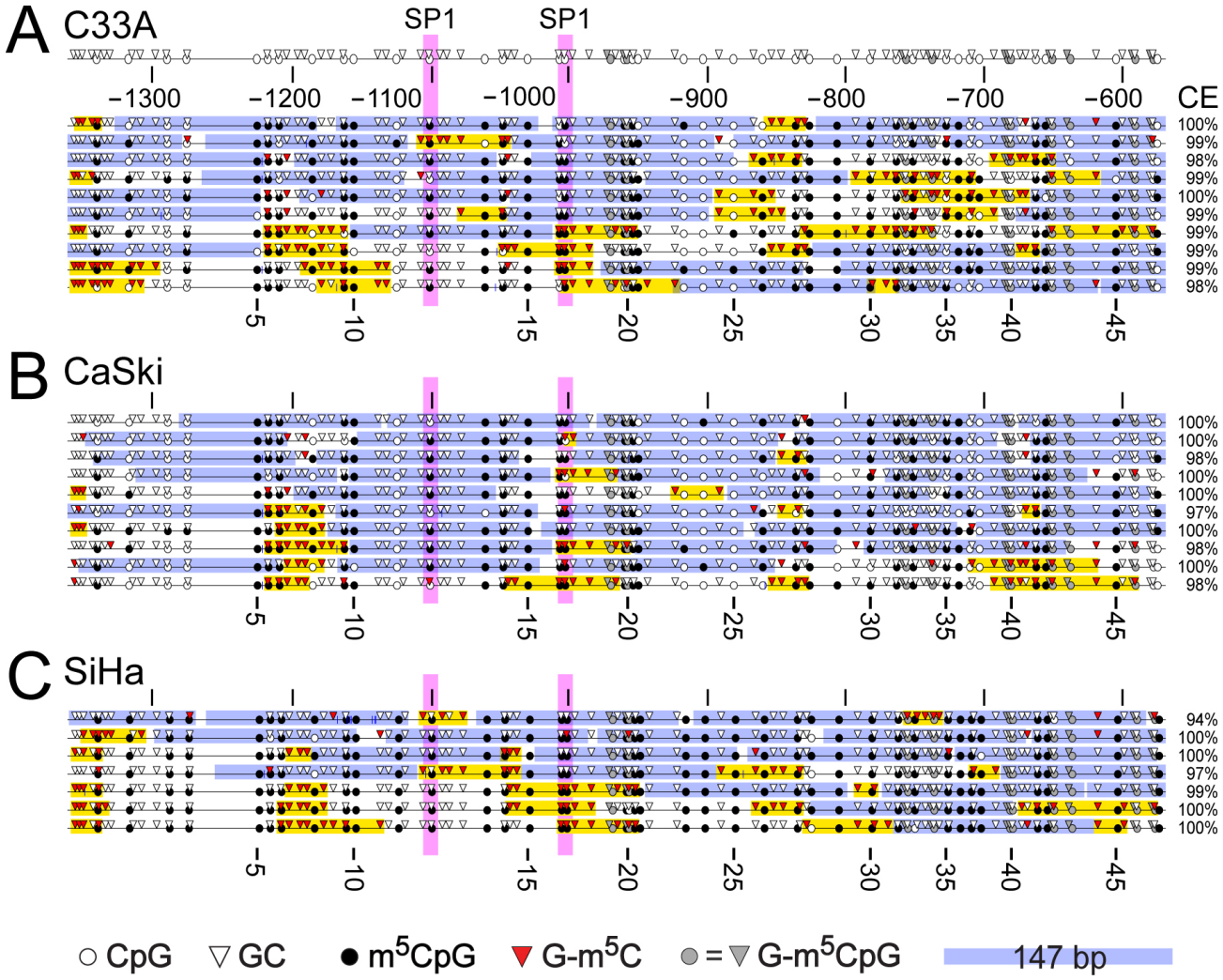

Supplemental Figure 1. *Dense DNA methylation of the distal upstream region of the WIF1 gene promoter in cervical cancer cell lines.* Nuclei from (*A*) C33A, (*B*) CaSki, and (*C*) SiHa cells were subjected to single-molecule MAPit methylation footprinting with M.CviPI. *WIF1* promoter coordinates (to scale) relative to the downstream TSS are shown over the top dataset. Each individually-cloned and -sequenced molecule is indicated by a horizontal line, with the bisulfite conversion efficiency (CE) for cytosines not in CpG or GC sites indicated at the right. Symbols indicating the status of methylation at all GC and sites are defined in the legend at the bottom of C of each dataset (only CpG sites numbered). Two putative SP1 binding sites are indicated at the top of A (pink). Consecutive G-m^{5}C (≥ 2 sites) flanked by ≥ 2 unmethylated GC sites indicate patches chromatin accessibility (yellow). Similarly, nucleosome-length protected patches of 147 bp (or less at either end of each molecule) are shaded blue. Methylated GCpG sites (G-m^{5}CpG; gray triangles) were excluded from patch designations as methylation by endogenous enzymes *versus* M.CviPI cannot be discerned.

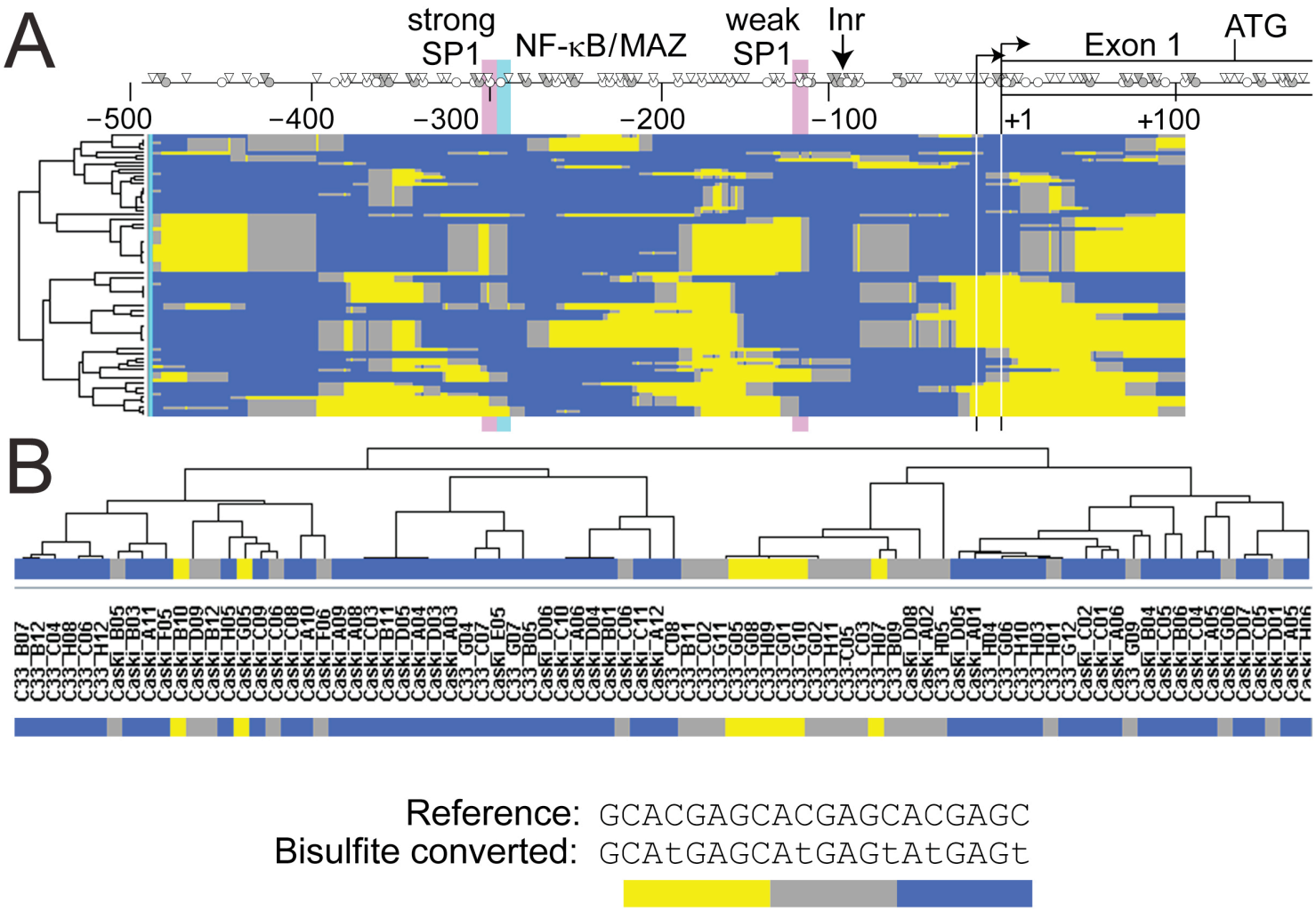

Supplemental Figure 2. *WIF1 gene promoter chromatin structure populates distinct clusters.* (*A*) Hierarchical clustering of three-color representation of methylation at GC sites. After conversion of GC methylation from −597 to +109 to mathematical values as defined in the Materials and Methods, molecules from C33 and SiHa cells were mixed and subjected to hierarchical clustering. (*B*) Enlargement of clustering root structure showing the cell type and name of individual molecules. Note that the majority of molecules from each cell type populate the same or adjacent clusters in the tree, indicating the presence of distinct and co-existing chromatin architectures in each cell type. The key for the visual representation of methylation status is shown at the bottom.

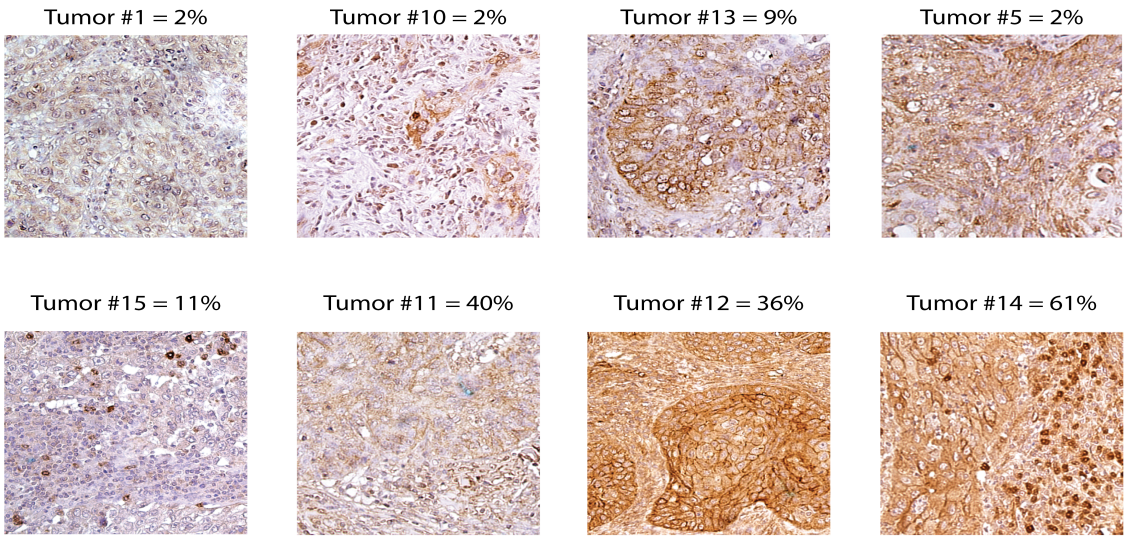

Supplemental Figure 3. *Immunohistochemical analysis of β-catenin expression in cervical SCC tissues.* Tumor tissue was sectioned and stained with anti-β-catenin antibody (Bethyl Labs, Montgomery TX; Cat# IHC00584). Sections were subsequently incubated with peroxidase-labeled secondary antibody and developed using DAB chromagen as outlined in Materials and Methods. Sections were subsequently counterstained with hematoxylin and semi-quantitatively scored for β-catenin staining. Shown are representative micrographs and the *WIF1* gene methylation as measured by pyrosequencing.

Scoring β-catenin expression in sections of 17 independent cervical SCC tumors indicated that all of these samples were either modestly or strongly positive for β-catenin staining. As 35.2% (6/17) of these tumors contain low levels (0-9%) *WIF1* methylation we conclude that there is no clear association between *WIF1* methylation and of β-catenin immunoreactivity in cervical SCC.